Sonolytic Oxidation of $Tc(IV)O_2nH_2O$ Nanoparticles to $Tc(VII)O_4$ in Aqueous Solution

M. Zakir[1*], T. Sekine[2]
[1] *Department of Chemistry, Hasanuddin University, Indonesia*
[2] *Graduate School of Science, Tohoku University, Sendai, Japan*

ARTICLE INFO

Article history:
Received 20 November 2009
Received in revised form 14 April 2010
Accepted 18 April 2010

Keywords:
Tc-nanoparticles
Sonolytic oxidation
Tc(IV), Tc(VII)

ABSTRACT

Sonolysis of a hydrosol of $TcO_2{\cdot}nH_2O$ was investigated in the Ar- or He-atmosphere. Colloidal $TcO_2{\cdot}nH_2O$ nanoparticles were irradiated with a 200 kHz and 1.25 W/cm^2 ultrasound. It was found that the $TcO_2{\cdot}nH_2O$ colloids dispersed in an aqueous solution (under Ar or He atmosphere) was completely dissolved by ultrasonic irradiation (200 kHz, 200 W). The original brownish black color of the suspension slowly disappeared leaving behind a colorless solution. This change suggests that oxidation of Tc(IV) to Tc(VII) takes place. The oxidation was almost complete during 30 minutes sonication time under argon atmosphere for initial concentration of 6.0E-5 M. Addition of *t*-butyl alcohol, an effective radical scavenger which readily reacts with OH radicals, supressed the dissolution of $TcO_2{\cdot}nH_2O$ colloids. This reaction indicates that $TcO_2{\cdot}nH_2O$ molecules are oxidized by OH radicals produced in cavitation bubbles

INTRODUCTION

The chemical effects of ultrasound derive primarily from acoustic cavitation, namely the formation, growth, and implosive collapse of tiny bubbles in the medium. Bubble collapse in liquids results in an enormous concentration of energy from the conversion of the kinetic energy of the liquid motion into heating of the contents of the bubble. The high local temperatures and pressures, combined with extraordinarily rapid cooling, provide a unique means for driving chemical reactions under extreme conditions [1].

The interactions of ultrasound in aqueous solution are often similar to those of ionizing radiation. For example, H_2 and H_2O_2 are formed [2], while H atoms and OH radicals can be traced by spin trapping [3]. However, dissolved substances often experience chemical changes which cannot be understood simply in terms of attack by H or OH radicals. A typical example is the production of hydrogen in aqueous solution of 2-propanol (< 0.1 M), where it was shown by isotopic labeling that the hydrogen originated mainly from the alcohol [4]. The effect was explained by a thermal dehydrogenation of 2-propanol as the alcohol evaporates into the cavitation bubbles, in which the chemical effects are initiated by the high temperatures produced in the adiabatic compression phase or collapse of the bubbles. These temperatures may amount to several thousands kelvin [5].

A number of metal nanoparticles have been prepared by means of ultrasonic irradiation. Some examples that can be cited here are colloidal gold nanoparticles [6,7], Au/Pd bimetal nanoparticles [8], Pt nanoparticles [9], Pd nanoparticles [10], and Ag nanoparticles [11]. It is believed that OH radical and H atoms are responsible in the preparation of those metal nanoparticles. Some metals, however, demonstrate special properties in which they can only be reduced sonolytically by appropriate reducing agents, for example Rh(III) was successfully reduced by transforming OH radicals into highly reducing radicals [12]. This phenomena might be valid to Tc where this metal could only be reduced by a specific reducing agent. Our initial experiment showed that Tc could not be reduced by the recommended reducing agents available currently in the literature [13].

In addition, a recent review describes that there is a considerable interest in the sonochemistry of aqueous solution from the point of view of environmental remediation [14], for instance to eliminate undesirable chemical compounds in hazardous waste treatment. Ultrasonic irradiation has been utilized in the past years as a novel advanced oxidation process to answer the growing need for lower levels of contaminants in wastewater

* Corresponding author.
E-mail address: muhammadzakir@gmail.com (M. Zakir)

[15]. Thus, the sonochemical method is expected to be promising in the handling of high level nuclear waste in the future, especially technetium [16]. However, there is a very limited literature concerning the redox properties of technetium under ultrasonic irradiation.

Understanding the sonolytically induced redox properties of technetium is very important in order to prepare Tc nanoparticles for pharmaceutical use and catalyst [17], and to properly handle this radionuclide in the environment. In addition, sonolytic effects can be easily controlled in the use of this method for specific purposes, for instance redox or dissolution reactions of radionuclides in the nuclear waste.

This paper describes the oxidation processes of $Tc(IV)O_2.nH_2O$ nanoparticles to aqueous solution of $Tc(VII)O_4^-$. The oxidation mechanism from Tc(IV) to Tc(VII) is discussed. It is expected that understanding on the sonolytic oxidation of Tc(IV) will facilitate the study of redox properties of technetium under sonication in the future.

EXPERIMENTAL METHODS

Irradiation system

Ultrasonic irradiation was carried out using an oscillator of 65 mm in diameter (Kaijo; MFG. No. 5N11) and an ultrasonic generator (Kaijo 4021type; frequency 200 kHz), which was operated at 200 W. The reaction vessel was mounted at a constant position. The bottom of the vessel was 4.0 mm distant from the top of the oscillator. A 10 ml of Ar- or He-saturated hydrosol containing $TcO_2{\cdot}nH_2O$ nanoparticles was sonicated in the water bath which was maintained at 20°C by a cold water circulation system (SCINICS CH-201). The reaction vessel was closed from the air during the irradiation in the Ar- or He- atmosphere. The sonication time was 5 – 90 min. A schematic illustration of the ultrasonic irradiation system was shown in Fig. 1. The temperature of targets was monitored with a thermometer dipped in the water bath.

Sample Preparation

Technetium(IV) oxide colloid hydrosol was prepared from bremsstrahlung irradiation of aqueous pertechnetate (TcO_4^-) solution. The colloid was separated from unreduced pertechnetate by ultrafiltration. Concentration of the hydrosol of $TcO_2{\cdot}nH_2O$ colloid stock is 1.24E-3 M. The sample for ultrasonic irradiation was prepared from the stock hydrosol by dilution with triply distilled water. Final concentration of the hydrosols were adjusted to the range of 1.0E-5 to 1.2E-4 M. The sample was poured into the sonication vials (10 ml in volume) and was bubbled with Ar, or He, respectively.

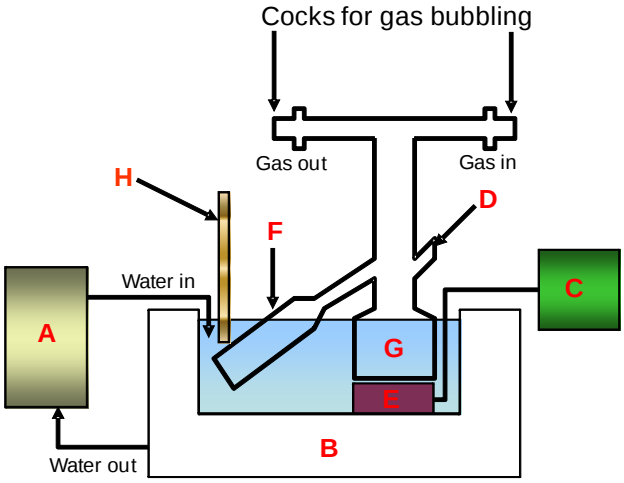

Fig. 1. Schematic view of the ultrasonic irradiation system.

A = water circulation and temperature control system (SCINICS CH-201); B = cooling water bath; C = ultrasonic generator (Kaijo 4021type; Lot. No. 54H6, Frequency: 200 kHz); D = silicon rubber septum; E = ultrasonic transducer (diameter: 65 mm; Kaijo; MFG. No. 89J5); F = quartz cell for UV-Vis measurement; G = glass reaction vessel; H = thermometer.

Determination of formation rate of OH radicals

The formation rate of H_2O_2 and OH radical during the sonolysis of the Ar-saturated, or He-saturated water were estimated by a method similar to Fricke dosimetry[18]: a 10 ml of Ar-saturated (and/or He) aqueous solution containing 50 mM $Fe(NH_4)_2(SO_4)_2$ and 0.8 N H_2SO_4 was irradiated and then the amount of Fe(III) ions (ε = 2194 $M^{-1}cm^{-1}$, λ = 304 nm) formed from the H_2O_2 and OH radical oxidation of Fe(II) was spectrophotometrically determined.

Technetium Analyses

The UV-visible spectra of Tc(VII) were recorded on a Shimadzu MultiSpec-1500 in the range from 190 to 800 nm. The concentration of pertechnetate was determined by the optical absorption (ε = 622 M^{-1} cm^{-1} at λ = 244 nm, and ε = 236 M^{-1} cm^{-1} at λ = 287 nm, where ε represents the molar absorption coefficient at the corresponding wavelength λ [19,20]. The fraction of $^{99}TcO_2{\cdot}nH_2O$ colloid in the sample is determined by imaging analysis of thin layer chromatography (TLC) plate. TLC was performed using Merk

60 F_{254} precoated silica gel plate (0.2 mm in thickness). Radioactivity of technetium-99 species on TLC-plate visualized with using an imaging plate (Fuji Photo Film, BAS-IP SR 2025) were analyzed by a Bio Imaging Analyzer (Fuji Photo Film, BAS-5000).

RESULTS AND DISCUSSION

Estimation of the production rate of OH radicals

The absorption spectra of formation of Fe(III) were recorded during the sonolysis of Ar- or He-saturated of Fe(II) aqueous solutions. The amount of Fe(III) ion was calculated by using the ε value = 2194 M^{-1} cm^{-1} at λ = 304 nm. The results were shown in Table 1.

Table 1. Results from the calculation of Fe^{3+} concentration in the sonolysis of Fe^{2+} aqueous solution under (a) Ar and (b) He atmosphere, respectively. The average of formation rates were 28.1±2.70 μM. min^{-1} under Ar, and 11.6±1.20 μM. min^{-1} under He, respectively.

(a) Argon atmosphere

Sonication time/min	$[Fe^{3+}]$ (M)	Rate (M. min^{-1})
0	0	0
5	1.60E-4	3.20E-5
10	2.96E-4	2.96E-5
15	4.34E-4	2.89E-5
20	5.56E-4	2.78E-5
25	6.59E-4	2.64E-5
30	7.23E-4	2.41E-5
	Average	2.81±0.27E-5 M. min^{-1}

(b) Helium atmosphere

Sonication time/min	$[Fe^{3+}]$ (M)	Rate (M. min^{-1})
0	0	0
5	4.79E-5	9.58E-6
10	1.08E-4	1.08E-5
15	1.78E-4	1.18E-5
20	2.50E-4	1.25E-5
25	3.08E-4	1.23E-5
30	3.78E-4	1.26E-5
	Average	1.16±0.12E-5 M. min^{-1}

The oxidation of Fe^{2+} by OH radicals can be simply written down as

$$Fe^{2+} + OH \rightarrow Fe^{3+} + OH^- \quad (1)$$

Hence, the amount of OH radicals formed in the sonolysis of water can be estimated from the amount of Fe^{3+} in the solutions. The rate of Fe(III) formation were found to be 28.1±2.70 μM. min^{-1} under argon, and 11.6±1.20 μM. min^{-1} under helium, respectively. Therefore, the OH formation rates of each gas condition in this experiment were estimated to be 28.1±2.70 μM.min^{-1} under argon, and 11.6±1.20 μM. min^{-1} under helium.

The OH-radical production depends on the nature of the operating gas. The temperature reached in the compressed bubble depends mainly on the ratio of specific heats C_p/C_v of the gas and its thermal conductivity. The presence of water vapour and of other polyatomic volatile components of the solution will depress the value of C_p/C_v below that of a pure monoatomic or diatomic gas. Any endothermic reaction will further depress this ratio as it acts to increase the apparent heat capacity. In the perfectly adiabatic limit, T_{max} and V_{min} of the collapsed bubble are linked by the expression $T_{max}/T_o=(V_o/V_{min})^{Cp/Cv-1}$, wherefrom it is seen that in a situation where C_p/C_v approaches unity, the temperature rise must be small even at high compression ratios [21]. Further, the higher the thermal conductivity, the more efficient the heat transfer out of the compressed bubble. The ratio C_p/C_v between He and Ar is almost the same (Table 2), but thermal conductivity of He is much higher than Ar, so that under He, the OH-radical yield is about three times lower than under argon atmosphere. The trend of increasing OH-radical yield with decreasing heat conductivity in the noble gases is well established [22, 23].

Tabel 2. Effect of saturating gases properties on OH formation rate in pure water

Saturating gas	OH formation rate[a] μM min^{-1}	Thermal conductivity (σ), milliwatt $m^{-1}K^{-1}$(300K)	Polytropic index, $\gamma = Cp/Cv$(25°C)
Helium	11.6±1.20	156.7	1.67
Argon	28.1±2.70	17.9	1.68

[a]Average value obtained from Table 1

This can be attributed to a difference of the effective maximum temperature in the collapsing bubbles. Because the thermal conductivity of He is larger than that of Ar, thermal transport effectively occurs from the bubbles to the surrounding liquid. Thus, cavitation bubbles filled with He should be cooler than those filled with Ar, resulting in the slower OH formation rate.

Sonication of aqueous solution of $TcO_2 \cdot nH_2O$ nanoparticles

Sonolysis of $TcO_2 \cdot nH_2O$ colloids dispersed in aqueous solution was investigated under Ar or He atmosphere. Gradual oxidation was observed from

the Tc(IV)$O_2 \cdot nH_2O$ colloid to TcO_4^-. The original brownish black color of the suspension disappeared leaving behind a colorless solution. The oxidation was completed during 30 minutes sonication time under argon atmosphere for initial concentration of 6.0 E-5 M as can be seen in the UV-Vis spectra (Fig. 2). Helium atmospheres did not show the same courses. It took 60 minutes to have the oxidation went to completion. The characteristics absorption peaks of pertechnetate were clearly appeared at the 30 min sonication. Fig. 2 shows the changes in the absorption spectra during sonication, both under Ar and He.

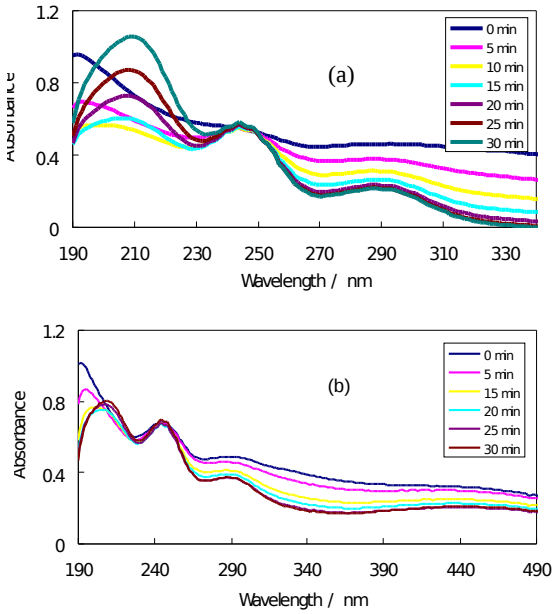

Fig. 2. Changes in the absorption spectra during sonication of $TcO_2.nH_2O$ colloids dispersed in aqueous solution. (a) Ar and (b) He. Cell length: 1 cm.

The amounts of Tc(IV)$O_2 \cdot nH_2O$ and Tc(VII)O_4^- in the samples were determined by thin layer chromatography (TLC). Imaging analysis of the TLC-plates of the samples clearly shows the disappearance of $TcO_2 \cdot nH_2O$ colloid spot on the plate after ultrasonic irradiation. The retardation factor (R_f) for Tc(IV) is 0 and Tc(VII) is 0.7, respectively. Both sample`s image and its Photostimulated Luminescence (PSL) spectra were recorded during the imaging analysis. The total activity before sonication was 17399 dpm, while after sonication was 17250 dpm. This suggests that Tc(IV)$O_2 \cdot nH_2O$ colloids were oxidized to Tc(VII)O_4^-.

Since $TcO_2 \cdot nH_2O$ used in the present study is a non-volatile compound, the solute does not pyrolyze in the cavitation bubbles. To confirm the reaction pathway, the effect of the radical scavenger, *t*-butyl alcohol ($(CH_3)_3COH$), on the rate of $TcO_2 \cdot nH_2O$ dissolution was investigated in an Ar atmosphere (Fig. 3). *t*-Butyl alcohol readily reacts with OH and H radicals [24, 25]. The production of TcO_4^- was considerably suppressed in the presence of *t*-butyl alcohol (an effective scavenger of OH radicals), indicating that Tc was oxidized by OH radicals produced in cavitation bubbles.

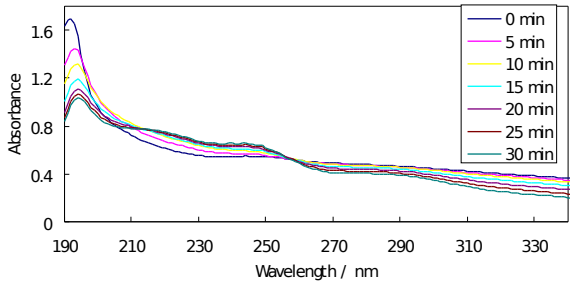

Fig. 3. Effects of radical scavenger addition (*t*-butyl alcohol) on the rate of decomposition of $TcO_2 \cdot nH_2O$. Ar-atmosphere, $[TcO_2 \cdot nH_2O]_0$ = 6 E -5 M.

The oxidation reaction of Tc must compete with the recombination reaction of OH radicals in the bulk solution region as follows:

$$OH + OH \rightarrow H_2O_2 \quad (2)$$

It should be recalled that H_2O_2 produced from the recombination of OH radicals is a nice oxidizing agent for $TcO_2 \cdot nH_2O$.

Mechanisms of sonolytic oxidation of $TcO_2 \cdot nH_2O$ nanoparticles

The mechanisms involved in the dissolution of colloidal $TcO_2 \cdot nH_2O$ nanoparticles should be considered with regard to the species generated from the water molecules by absorption of ultrasound. The species, as mentioned above, are originated from the following reactions.

$$H_2O))) \rightarrow H + OH \quad (3)$$
$$H + OH \rightarrow H_2O \quad (4)$$
$$H + H \rightarrow H_2 \quad (5)$$
$$OH + OH \rightarrow H_2O_2 \quad (6)$$

It has been proposed that during the sonochemical treatments of many organic compounds in water [23,26], the oxidative decomposition generally proceeds via the reaction with OH radicals which are formed from water pyrolysis in the collapsing hot bubbles (3). Particularly in the case of volatile or hydrophobic compounds, the decomposition proceeds not only via OH radicals reaction but also via a direct pyrolysis reaction in the collapsing hot bubbles and the hot interface region [23,26].

Cavitation near extended liquid-solid interfaces is very different from cavitation in pure liquids. Near a solid surface, bubble collapse becomes nonspherical, driving high-speed jets of liquid into the surface and creating shockwave damage to the surface. Because most of the available energy is transferred to the accelerating jet, rather than the bubble wall itself, this jet can reach velocities of hundreds of meters per second. In addition, shockwaves created by cavity collapse in the liquid may also induce surface damage and the fragmentation of brittle materials.

The impingement of microjets and shockwaves on the surface creates the localized erosion responsible for ultrasonic cleaning and many of the sonochemical effects on heterogeneous reactions. The importance of this process to corrosion and erosion phenomena of metals and machinery has been thoroughly reviewed elsewhere [27].

Those effects mentioned above may cause the destruction of the passivating film on the surface of $TcO_2{\cdot}nH_2O$ nanoparticles and, accordingly, increase the rate of metal dissolution. Consequently, it seems that the dissolution of colloidal $TcO_2{\cdot}nH_2O$ nanoparticles might take place in two steps. The first step is the state change of $TcO_2{\cdot}nH_2O$ from the solid state into the solution state. The next step is a direct oxidation of Tc(IV) species to Tc(VII) species. Species generated from the water pyrolysis in the hot cavitation bubbles (or their recombination products) might be involved in the oxidation processes (3-6).

In summary, the dissolution mechanism of colloidal $TcO_2{\cdot}nH_2O$ nanoparticles by ultrasonic irradiation could be proposed as follows.

First step: destruction of $TcO_2{\cdot}nH_2O$ by shock waves generated from cavity collapses.

$$TcO_2{\cdot}nH_2O \quad))) \rightarrow TcO_2 + nH_2O \qquad (7)$$

$$TcO_2(s) \quad))) \rightarrow TcO_2(aq) \qquad (8)$$

Second step: oxidation of Tc(IV) species by either OH radicals or their recombination products.

(1) Water pyrolysis in the hot cavitation bubble (Reaction 3)
(2) Recombination of radicals (Reaction 6)
(3) Oxidation of Tc(IV) to Tc(VII) by OH radicals

Triggering reaction:

$$2\ Tc(IV) + 2\ {\cdot}OH \rightarrow Tc(V) + Tc(V) + 2\ OH^- \qquad (9)$$

Disproportionation reactions:

$$Tc(V) + Tc(V) \rightarrow Tc(IV) + Tc(VI) \qquad (10)$$

$$Tc(VI) + Tc(VI) \rightarrow Tc(V) + Tc(VII) \qquad (11)$$

(4) Oxidation of Tc(IV) by H_2O_2

$$Tc(IV) + 3\ H_2O_2 \rightarrow Tc(VII) + 3\ OH^- + 3\ {\cdot}OH \qquad (12)$$

CONCLUSIONS

$TcO_2{\cdot}nH_2O$ colloids dispersed in an aqueous solution, under Ar or He atmosphere, was completely dissolved by ultrasonic irradiation (200 kHz, 200 W), and TcO_4^- was eventually produced. The production of TcO_4^- was considerably suppressed in the presence of *t*-butyl alcohol (an effective scavenger of OH radicals), indicating that Tc was oxidized by OH radicals produced in cavitation bubbles. The formation rate of TcO_4^- under He atmosphere was slower than that under Ar atmosphere.

REFERENCES

1. K.S. Suslick, Science **247** (1990) 1439.
2. X. Fang, G. Mark, C. Von Sonntag, Ultrason. Sonochem **3** (1996) 57.
3. K. Makino, M.M. Mossoba, P. Riesz, J. Phys. Chem. **87** (1983) 1369.
4. M. Anbar, I.J. Pecht, J. Phys. Chem. **68** (1964) 1462.
5. B.E. Noltingk, E.A. Neppiras, Proc. Phys. Soc. London B **36** (1950) 674.
6. K. Okitsu, A. Yue, S. Tanabe, H. Matsumoto, Y. Yobiko, Langmuir **17** (2001) 7717.
7. J.E. Park, M. Atobe, T. Fuchigami, Ultrason. Sonochem **13** (2006) 674.
8. Y. Mizukoshi, T. Fujimoto, Y. Nagata, R. Oshima, Y, Maeda, J. Phys. Chem. B **104** (2000) 6028.
9. T. Nakagawa, H. Nitani, S. Tanabe, K. Okitsu, S. Seino, Y. Mizukoshi, T.A. Yamamoto, Ultrason. Sonochem **12** (2005) 249.
10. Y. Mizukoshi, R. Oshima, Y. Maeda, Y. Nagata, Langmuir **15** (1999) 2733.
11. Y. Mizukoshi, E. Takagi, H. Okuno, R.Oshima, Y. Maeda, Y. Nagata, Ultrason. Sonochem. **8** (2001) 1.
12. K. Okitsu, Y. Mizukoshi, H. Bandow, Y. Maeda, Y. Yamamoto, Y. Nagata, Ultrason. Sonochem. **3** (1996) 1.
13. M. Zakir, Ph.D. Thesis, Tohoku University, Sendai, Japan (2006).

14. R. Kidak, N.H. Ince, Ultrason. Sonochem. **13** (2006) 195.
15. Z. Guo, et al., Ultrason. Sonochem. **13** (2006) 471.
16. J.E.S. Cziganny, M. Flury, J.S. Harsh, Environ. Sci. Technol. **39** (2005) 1506.
17. K. Schwochau, *Technetium: Chemistry and Radiopharmaceutical Applications*, Wiley-Vch, Weinheim, Germany (2000).
18. Y. Nagata, Y. Mizukoshi, K. Okitsu, Y. Maeda, Radiat. Res. **146** (1996) 333.
19. L. Heller-Grossman, S. Abrashkin A. Shafferman, M.A. Davis,. R.A. Taube, Int. J. Appl. Radiat. Isotopes **32** (1981) 501.
20. K.B. Said, Y. Seimbille, M. Fattahi, C. Houee-Lévin, J.C. Abbé, Appl. Radiat. Isot. **54** (2001) 45.
21. W.B. McNamara III, Y.T. Didenko, K.S. Suslick, Nature **401** (1999) 772.
22. A. Henglein, Naturwiss **43** (1956) 277.
23. I. Hua, R.H. Hochemer, M. Hoffmann, J. Phys. Chem. **99** (1995) 2335.
24. M. Anbar, P. Neta, Int. J. Appl. Radiat. Isotop. **18** (1967) 493
25. P. Neta, R.W. Fessenden, R.H. Schuler, J. Phys. Chem. **75** (1971) 1654.
26. A.J. Colussi, L.K. Weavers, M. Hoffmann, J. Phys. Chem. A **102** (1992) 6927.
27. K.S. Suslick, G. J. Price, Annu. Rev. Mater. Sci. **29** (1999) 295.